PART II

# THE INTERPRETATION OF MAGNETOGRAPH RESULTS – THE FORMATION OF ABSORPTION LINES IN A MAGNETIC FIELD

# THE INTERPRETATION OF MAGNETOGRAPH RESULTS: THE FORMATION OF ABSORPTION LINES IN A MAGNETIC FIELD

J. O. STENFLO

*Astronomical Observatory, Lund, Sweden*

**Abstract.** The theory of line formation in a magnetic field is reviewed. It is shown how the formulations by Unno, Beckers, Stepanov and Rachkovsky are related to each other. The general treatment of true absorption, anomalous dispersion, radiative scattering and level-crossing interference is discussed. Special attention is paid to the inhomogeneous nature of the solar atmosphere. The properties of magnetic filaments are reviewed. It is shown how a filamentary structure will drastically influence the interpretation of magnetograph observations. The treatment of line formation in a turbulent magnetic field is also discussed.

The fine structure of the solar atmosphere will influence different types of magnetographs in entirely different ways. The relation between the observed magnetic field and the resolution of the instrument is discussed for a Babcock-type, Evans-type and a transversal magnetograph. Finally some suggestions for future work in this field are listed.

## 1. Introduction

The most important method to determine solar magnetic fields is to observe the Zeeman effect in the solar atmosphere. The polarization in magnetic-sensitive spectral lines can be analysed by sophisticated methods, and from the relative intensities and displacements of the differently polarized line components one can draw conclusions about the magnetic field at the level in the solar atmosphere where the spectral line is formed.

The main trouble in the interpretation of magnetograph observations has not been that we do not know enough about line formation in a magnetic field; it has been our lack of knowledge of the fine structure of the field. The magnetograph readings have been interpreted in terms of a homogeneous magnetic field although it has been completely clear that most of the magnetic features have not been resolved.

There are however a great number of unsolved problems in the basic theory of line formation in a magnetic field. And this theory forms the general basis for all interpretations of what is measured with a magnetograph. Before we can present a general formulation of the radiative transfer problem in a magnetic field we have to start with a suitable representation of polarized light.

## 2. Representation of Polarized Light

The vibration of the electrical vector of polarized light propagating along the $z$-axis in an $xyz$ coordinate system can be described by

$$\xi_x = \xi_1 \cos(\omega t - \varepsilon_1)$$

and (1)

$$\xi_y = \xi_2 \cos(\omega t - \varepsilon_2),$$

*Howard (ed.), Solar Magnetic Fields*, 101–129. *All Rights Reserved.*

where $\xi_x$ and $\xi_y$ are the components of the vibration along the $x$ and $y$ axis, and $\omega$ is the circular frequency. The four constants $\xi_1$, $\xi_2$, $\varepsilon_1$, and $\varepsilon_2$ are sufficient to define the state of polarization.

It is convenient to describe the polarization by means of a complex vector **m**. Let **e** and **e**′ be complex orthogonal unit vectors. Then

$$\mathbf{e}\cdot\mathbf{e}^* = \mathbf{e}'\cdot\mathbf{e}'^* = 1 \quad \text{and} \quad \mathbf{e}\cdot\mathbf{e}'^* = 0\,, \tag{2}$$

where **e*** denotes the conjugate form of **e**. The polarization vector **m** can be written

$$\mathbf{m} = E\mathbf{e} + E'\mathbf{e}'\,, \tag{3}$$

where $E$ and $E'$ are the complex amplitudes of the electric vector. If we choose a system in which **e** and **e**′ represent linear polarization, e.g. $\mathbf{e}=\hat{x}$ and $\mathbf{e}'=\hat{y}$, $\hat{x}$ and $\hat{y}$ being real unit vectors along the $x$ and $y$ axis, the vibration in (1) can be represented by (3) if we put $E=\xi_1 e^{-i\varepsilon_1}$ and $E'=\xi_2 e^{-i\varepsilon_2}$. The time-dependent factor $e^{i\omega t}$ is ignored as it is of no interest for the polarization. If $e^{i\omega t}$ is included, we obtain (1) by taking the real part of **m**.

Polarized light can be completely described by the four Stokes parameters $I_1$, $I_2$, $U$ and $V$.

$$\begin{aligned} I_1 &= \overline{EE^*}\,,\\ I_2 &= \overline{E'E'^*}\,,\\ U &= \sqrt{2}\,\mathrm{Re}\,(\overline{EE'^*})\,,\\ V &= -\sqrt{2}\,\mathrm{Im}\,(\overline{EE'^*})\,. \end{aligned} \tag{4}$$

A line above the symbols means a time average. Re and Im mean that the real and imaginary part of the quantity is taken, respectively.

In our system of linear polarization, (4) can be rewritten in the form

$$\begin{aligned} I_1 &= \overline{\xi_1^2}\,,\\ I_2 &= \overline{\xi_2^2}\,,\\ U &= \sqrt{2}\,\overline{\xi_1\xi_2\cos(\varepsilon_1-\varepsilon_2)}\,,\\ V &= \sqrt{2}\,\overline{\xi_1\xi_2\sin(\varepsilon_1-\varepsilon_2)}\,. \end{aligned} \tag{5}$$

The parameters $U$ and $V$ used by Chandrasekhar (1950) and Unno (1956) are larger than ours by a factor of $\sqrt{2}$. However, by defining the parameters as in (4) and (5), the matrices appearing in the theory will be symmetric or anti-symmetric.

In many papers the parameters $I$ and $Q$ are used instead of $I_1$ and $I_2$. We have the relations $I=I_1+I_2$ and $Q=I_1-I_2$.

A compact form of representation of polarized light is by means of a four-dimensional vector

$$\mathbf{I} = \begin{pmatrix} I_1 \\ I_2 \\ U \\ V \end{pmatrix}. \tag{6}$$

The values of the Stokes parameters depend on the choice of the vector system $(\mathbf{e}, \mathbf{e}')$. Suppose that $\mathbf{e}$ and $\mathbf{e}'$ as before represent linear polarization along the $x$ and $y$ axis, and that we make a rotation of the coordinate system by an angle $\varphi$ in the anti-clockwise direction. The unit vectors in the new system are

$$\begin{aligned}\mathbf{e}_1 &= \mathbf{e}\cos\varphi + \mathbf{e}'\sin\varphi,\\ \mathbf{e}_1' &= -\,\mathbf{e}\sin\varphi + \mathbf{e}'\cos\varphi.\end{aligned} \tag{7}$$

The Stokes parameters in the new system are obtained by a linear transformation

$$\mathbf{I}^{(1)} = \mathbf{L}_1\mathbf{I}. \tag{8}$$

$$\mathbf{L}_1 = \begin{pmatrix} p & 1-p & q & 0\\ 1-p & p & -q & 0\\ -q & q & 2p-1 & 0\\ 0 & 0 & 0 & 1\end{pmatrix}, \tag{9}$$

where

$$\begin{aligned}p &= \cos^2\varphi,\\ q &= \frac{1}{\sqrt{2}}\sin 2\varphi.\end{aligned} \tag{10}$$

The unit vectors describing mutually orthogonal elliptical polarization can be written

$$\begin{aligned}\mathbf{e}_2 &= \mathbf{e}\cos\varphi + \mathbf{e}'\, i\sin\varphi,\\ \mathbf{e}_2' &= \mathbf{e}\, i\sin\varphi + \mathbf{e}'\cos\varphi,\end{aligned} \tag{11}$$

where $\mathbf{e}$ and $\mathbf{e}'$ still represent linear polarization. The principal axis of the ellipses are along $\mathbf{e}$ and $\mathbf{e}'$. The ratio between the axis of the ellipses is tan $\varphi$ or ctn $\varphi$. The linear transformation between the two systems in (11) is

$$\mathbf{L}_2 = \begin{pmatrix} p & 1-p & 0 & q\\ 1-p & p & 0 & -q\\ 0 & 0 & 1 & 0\\ -q & q & 0 & 2p-1\end{pmatrix}. \tag{12}$$

The inverse transformation is determined by

$$\mathbf{L}_{1,2}^{-1} = \mathbf{L}_{1,2}^{T}, \tag{13}$$

where $\mathbf{L}^T$ is the transpose of $\mathbf{L}$.

## 3. Radiative Transfer in a Magnetic Field

### 3.1. True Absorption

This is the case for which the theory is most developed. The transfer equation can conveniently be written using the compact matrix formulation.

$$\cos\theta\,\frac{d}{d\tau}\mathbf{I} = (\mathbf{1} + \boldsymbol{\eta})\,(\mathbf{I} - \mathbf{B}). \tag{14}$$

$\theta$ is the heliocentric angle, and $\tau$ is the optical depth related to the continuous absorption coefficient. **1** is the unit matrix. The intensity vector **I** is defined by (6) and the source function vector by

$$\mathbf{B} = \begin{pmatrix} B/2 \\ B/2 \\ 0 \\ 0 \end{pmatrix}, \tag{15}$$

$B$ being the Planck function.

In the system of Stokes parameters (5), the absorption matrix can be written

$$\boldsymbol{\eta} = \begin{pmatrix} a_+ & 0 & b & c \\ 0 & a_- & b & c \\ b & b & (a_+ + a_-)/2 & 0 \\ c & c & 0 & (a_+ + a_-)/2 \end{pmatrix} \tag{16}$$

where

$$a_\pm = \tfrac{1}{2}[\eta_p - \tfrac{1}{2}(\eta_r + \eta_b)] \sin^2\gamma (1 \pm \cos 2\chi) + \tfrac{1}{2}(\eta_r + \eta_b), \tag{17}$$

$$b = \frac{1}{2\sqrt{2}} [\eta_p - \tfrac{1}{2}(\eta_r + \eta_b)] \sin^2\gamma \sin 2\chi, \tag{18}$$

$$c = \frac{1}{2\sqrt{2}} (\eta_r - \eta_b) \cos\gamma. \tag{19}$$

$\eta_{p,r,b}$ denotes the ratio between the coefficients of line absorption and continuous absorption for the three Zeeman components. Index $p$ refers to transitions for which the change in magnetic quantum number $\Delta m = 0$. For $r$, $\Delta m = -1$, and for $b$, $\Delta m = 1$. We have

$$\begin{aligned} \eta_p &= \eta_0 H(\alpha, v), \\ \eta_r &= \eta_0 H(\alpha, v - v_H), \\ \eta_b &= \eta_0 H(\alpha, v + v_H), \end{aligned} \tag{20}$$

where $\eta_0$ is the ratio between the line absorption coefficient at the line centre and the continuous absorption coefficient. The function $H$ giving the form of the absorption profile is usually assumed to be a Voigt function.

$$\alpha = \gamma_d / \Delta\lambda_D, \tag{21}$$

$\gamma_d$ being the damping constant and $\Delta\lambda_D$ the Doppler width.

$$v = \frac{\Delta\lambda}{\Delta\lambda_D} \tag{22}$$

and

$$v_H = \frac{\Delta\lambda_H}{\Delta\lambda_D}. \tag{23}$$

https://doi.org/10.1017/S0074180900022476 Published online by Cambridge University Press

The Zeeman splitting is determined by

$$\Delta\lambda_H = 4.67 \times 10^{-13}\, \lambda^2 g H\,. \tag{24}$$

$H$ is the magnetic field strength in $G$ and $g$ the Landé factor. The wavelength should be given in Å. Doppler shifts can also easily be included in (20).

The geometry of the system to which $\boldsymbol{\eta}$ in (16) refers is described by Figure 1. $\gamma$ is the angle between the magnetic field and the line of sight and $\chi$ the azimuth angle of the field vector.

With the formulation of the transfer equations given by (14)–(19) we are not restricted to the case of homogeneous magnetic fields. The field may exhibit any variation in magnitude and direction with depth in the solar atmosphere. The ab-

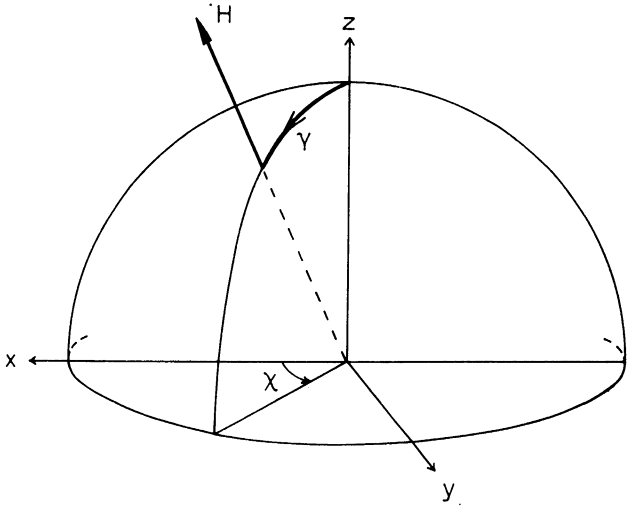


Fig. 1. Geometry for the case of true absorption. The $z$-axis is assumed to be directed along the line of sight. $\chi$ is the azimuth angle of the magnetic-field vector, $\gamma$ the angle between the field and the line of sight.

sorption coefficients, line broadening mechanisms and radial velocities may also have any variation with depth.

With (14)–(19) one can calculate the polarization of the emerging radiation for inhomogeneous fields and different model atmospheres. This was first done by Beckers (1969a, b). His formulation of the transfer equations is equivalent to ours. Beckers integrated the four coupled differential equations by means of a Runge-Kutta technique.

The absorption matrix can be written in many different ways depending on what system of Stokes parameters has been used. Transformations from one system to another can be made by means of the matrices $\mathbf{L}_{1,2}$ given by (9) and (12). If we

https://doi.org/10.1017/S0074180900022476 Published online by Cambridge University Press

denote matrices in the new system with a prime, we have

$$\cos\theta \frac{d}{d\tau} \mathbf{I}' = \mathbf{L}_{1,2} (\mathbf{1} + \boldsymbol{\eta}) \mathbf{L}_{1,2}^{-1} (\mathbf{I}' - \mathbf{B}'). \tag{25}$$

It is easy to show that the source function $\mathbf{B}$ is not changed by the transformations $\mathbf{L}_{1,2}$. Hence (25) can be written

$$\cos\theta \frac{d}{d\tau} \mathbf{I}' = (\mathbf{1} + \boldsymbol{\eta}') (\mathbf{I}' - \mathbf{B}), \tag{26}$$

where

$$\boldsymbol{\eta}' = \mathbf{L}_{1,2} \boldsymbol{\eta} \mathbf{L}_{1,2}^{T}, \tag{27}$$

and (13) has been used.

By applying the transformation $\mathbf{L}_1$ with $\varphi$ in (10) equal to $\chi$, we rotate the coordinate system in Figure 1 so that the magnetic field vector will be in the $xz$-plane. Then we obtain the absorption matrix in the same system as that used by Unno (1956) when he first developed the theory of line formation in a magnetic field. Of course we also obtain Unno's equations directly by putting $\chi = 0$ in (17) and (18). The Unno formulation is unable to treat line formation in magnetic fields of variable azimuth.

If we in (27) let $\boldsymbol{\eta}$ be the Unno absorption matrix and use the $\mathbf{L}_2$ transformation (12) with $\varphi$ determined by

$$\begin{aligned} \operatorname{ctn} \varphi = \{&[\eta_p - \tfrac{1}{2}(\eta_r + \eta_b)] \sin^2\gamma \\ &\pm \sqrt{[\eta_p - \tfrac{1}{2}(\eta_r + \eta_b)]^2 \sin^4\gamma + (\eta_r - \eta_b)^2 \cos^2\gamma}\}/(\eta_r - \eta_b) \cos\gamma, \end{aligned} \tag{28}$$

the absorption matrix $\boldsymbol{\eta}$ will be diagonalized.

$$\boldsymbol{\eta}' = \begin{pmatrix} \eta_+ & 0 & 0 & 0 \\ 0 & \eta_- & 0 & 0 \\ 0 & 0 & (\eta_+ + \eta_-)/2 & 0 \\ 0 & 0 & 0 & (\eta_+ + \eta_-)/2 \end{pmatrix}. \tag{29}$$

$$\begin{aligned} \eta_\pm = &\tfrac{1}{2} [\eta_p - \tfrac{1}{2}(\eta_r + \eta_b)] \sin^2\gamma + \tfrac{1}{2}(\eta_r + \eta_b) \\ &\pm \tfrac{1}{2} \sqrt{[\eta_p - \tfrac{1}{2}(\eta_r + \eta_b)]^2 \sin^4\gamma + (\eta_r - \eta_b)^2 \cos^2\gamma}. \end{aligned} \tag{30}$$

It is seen that

$$\eta_+ + \eta_- = a_+ + a_-, \tag{31}$$

where $a_\pm$ are given by (17) for $\chi = 0$.

The diagonal form (29) is by far the most suitable for calculations of the polarization of the emerging radiation, since the four transfer equations are independent of each other and can be solved by means of all methods that have been developed for unpolarized radiation. Unfortunately the matrix does not diagonalize for arbitrary values of the azimuth $\chi$.

If we assume that the radiation becomes unpolarized as $\tau \to \infty$ the parameters $U'$

and $V'$ must be $\equiv 0$ throughout the atmosphere. This is so because the source function is zero for $U'$ and $V'$. With this boundary condition the four transfer equations reduce to the two

$$\cos\theta \frac{d}{d\tau} I_\pm = (1 + \eta_\pm)\left(I_\pm - \frac{B}{2}\right). \tag{32}$$

Here we have used the notation $I_+$ and $I_-$ instead of $I_1'$ and $I_2'$.

When Stepanov (1958a, b) independently of Unno first developed the theory of line formation in a magnetic field he started by calculating the line absorption coefficients from the classical magneto-optical theory. This yielded $\eta_\pm$ in (30). Stepanov (1958a) found that $\eta_+$ and $\eta_-$ correspond to absorption of two mutually orthogonal beams $I_\pm$. An atmosphere that absorbs $I_+$ is completely transparent for $I_-$ and vice versa. $I_+$ and $I_-$ cannot interfere (Chandrasekhar, 1950). In this way Stepanov (1958b) arrived at the Equations (32).

Rachkovsky (1961a) showed that Stepanov's Equations (32) could be deduced from Unno's equations but that the two more equations in (29) had to be added to make the system fully equivalent to that of Unno (Rachkovsky, 1961b).

There is one important restriction which we must notice when we use (32). When solving (32) the system for the Stokes parameters must be the same for all $\tau$, which means that the transformation determined by $\operatorname{ctn}\varphi$ in (28) must be independent of depth. This means in the general case that the magnetic field has to be homogeneous and that the Voigt functions in (20) are independent of $\tau$. $\eta_0$ may however have any variation with $\tau$.

In the case of a purely longitudinal ($\gamma = 0°$) or transversal ($\gamma = 90°$) field with constant azimuth, however, any variations in the field strength, radial velocity and line broadening parameters are allowed for.

Stepanov (1958b) gave analytical solutions of (32) and calculated the profile of the line Fe I 6173 Å in sunspots. Mattig (1966) suggested numerical solutions of (32) using different model atmospheres. Such numerical integrations of (32) were made by Moe (1968), Moe and Maltby (1968), Evans (1968, 1969a, b), and Evans and Dreiling (1969).

Having obtained a solution $\mathbf{I}'$ for the emerging radiation in Stepanov's system we can easily transform it to the common Stokes parameters $\mathbf{I}$ by

$$\mathbf{I} = \mathbf{L}_2^T \mathbf{I}'. \tag{33}$$

If $U' = V' = 0$ we find

$$\begin{aligned} I &= I_+ + I_-, \\ Q &= (I_+ - I_-)\cos 2\varphi, \\ U &= 0, \\ V &= (I_+ - I_-)\, 2^{-1/2} \sin 2\varphi, \end{aligned} \tag{34}$$

where $\varphi$ is determined by (28). Note that $U$ and $V$ are defined as in (5) and are smaller than Chandrasekhar's (1950) $U$ and $V$ by a factor of $\sqrt{2}$.

### 3.2. Anomalous dispersion

In the preceding section we have ignored the variation of the refractive index $n$ within the line. In a magnetic field this effect may be of some importance, however, since the refractive index will be different for the differently polarized components of a Zeeman-split line. Hence we obtain different retardations of the components. In a longitudinal magnetic field there will be relative retardations between the left- and right-hand circular polarizations which causes a rotation of the polarization ellipse. This is the *Faraday rotation* or *Macaluso-Corbino* effect. In the case of a transversal magnetic field we have instead linear birefringence resulting in the so-called *Voigt effect* (Born, 1965). In the general case we have *elliptical birefringence*.

The refractive index $n$ in the line in the absence of Doppler broadening is determined by (Beckers, 1969a)

$$n - 1 = \frac{\kappa_0 \lambda}{4\pi^{3/2} H(\alpha, 0)} \frac{v}{v^2 + \alpha^2}, \tag{35}$$

where $v$ and $\alpha$ are given by (22) and (21). $\kappa_0$ is the line absorption coefficient at the centre of the line, and $H(\alpha, 0)$ is the Voigt function for $v=0$. Including Doppler broadening, we obtain (Born, 1965; Beckers, 1969a; Rachkovsky, 1962a)

$$n - 1 = \frac{\kappa_0 \lambda}{2\pi H(\alpha, 0)} F(\alpha, v), \tag{36}$$

where

$$F(\alpha, v) = \frac{1}{2\pi} \int_{-\infty}^{+\infty} \frac{u}{u^2 + \alpha^2} e^{-(u-v)^2} \, \mathrm{d}u. \tag{37}$$

Rachkovsky (1962a) expanded $F(\alpha, v)$ in a power series

$$F(\alpha, v) \approx \sum_{i=0}^{3} \alpha^i F_i(v). \tag{38}$$

The functions $F_i$ have been tabulated by Beckers (1969a).

Anomalous dispersion can be included in the transfer equation (14) by writing the absorption matrix $\boldsymbol{\eta}$ as

$$\boldsymbol{\eta} = \boldsymbol{\eta}_a + \boldsymbol{\eta}_\delta, \tag{39}$$

where $\boldsymbol{\eta}_a$ is our earlier absorption matrix given by (16)–(19), while

$$\boldsymbol{\eta}_\delta = \begin{pmatrix} 0 & 0 & d & \frac{1}{\sqrt{2}} e \sin 2\chi \\ 0 & 0 & -d & -\frac{1}{\sqrt{2}} e \sin 2\chi \\ -d & d & 0 & -e \cos 2\chi \\ -\frac{1}{\sqrt{2}} e \sin 2\chi & \frac{1}{\sqrt{2}} e \sin 2\chi & e \cos 2\chi & 0 \end{pmatrix}, \tag{40}$$

where

$$d = \frac{1}{\sqrt{2}} (\delta_r - \delta_b) \cos\gamma, \tag{41}$$

$$e = -\left[\delta_p - \tfrac{1}{2}(\delta_r + \delta_b)\right] \sin^2\gamma, \tag{42}$$

$$\begin{aligned} \delta_p &= \eta_0 F(\alpha, v), \\ \delta_r &= \eta_0 F(\alpha, v - v_H), \\ \delta_b &= \eta_0 F(\alpha, v + v_H). \end{aligned} \tag{43}$$

The corresponding expressions by Beckers (1969a, b) are too small by a factor of $2\,H(\alpha, 0)$.

By applying on $\boldsymbol{\eta}_\delta$ the transformation $\mathbf{L}_1$ as in (27) with $\varphi$ in (11) $= \chi$, we obtain the same matrix as that found by Rachkovsky (1962a, b, 1967d) when he developed the theory of anomalous dispersion in stellar atmospheres. This matrix is also obtained by putting $\chi = 0$ in (40).

Generally the effect of elliptical birefringence in stellar atmospheres is small and can in most cases be neglected. The Faraday rotation is limited because the matrix coefficients $\eta_i$ and $\delta_i$ in (20) and (43) are of the same order of magnitude. The rotation is proportional to the optical thickness $\Delta\tau$ of the line-forming layer. For $\Delta\tau = 1$ it is well below one radian. Radiation for which the rotation is larger than one radian is simply so much absorbed that it does not escape from the atmosphere. The effects of anomalous dispersion are thus much smaller than suggested by Kai (1968) and cannot explain the rapid changes in the field azimuth observed by Severny (1964, 1965).

The solution of the transfer equations for a homogeneous magnetic field with $\chi = 0$, assuming a Milne-Eddington atmosphere and a linear Planck function

$$B = B_0 (1 + \beta_0 \tau), \tag{44}$$

but including anomalous dispersion, was found by Rachkovsky (1962b, 1967d). If quantities with index zero refer to the continuum, the solution is

$$\begin{aligned} r_I(0, \theta) &= \frac{I_0(0, \theta) - I(0, \theta)}{I_0(0, \theta)} = \frac{\beta_0 \cos\theta}{1 + \beta_0 \cos\theta} \\ &\quad \times \left[1 - \frac{\eta_I(\eta_I^2 + l^2)}{\eta_I^2(\eta_I^2 + l^2 - m^2) - \alpha^2}\right], \\ r_Q(0, \theta) &= \frac{Q_0(0, \theta) - Q(0, \theta)}{I_0(0, \theta)} = \frac{\beta_0 \cos\theta}{1 + \beta_0 \cos\theta} \frac{\eta_I^2 (a_+ - a_-)/2 - \alpha e}{\eta_I^2(\eta_I^2 + l^2 - m^2) - \alpha^2}, \\ r_U(0, \theta) &= \frac{U_0(0, \theta) - U(0, \theta)}{I_0(0, \theta)} = -\frac{\beta_0 \cos\theta}{1 + \beta_0 \cos\theta} \frac{\eta_I \beta}{\eta_I^2(\eta_I^2 + l^2 - m^2) - \alpha^2}, \\ r_V(0, \theta) &= \frac{V_0(0, \theta) - V(0, \theta)}{I_0(0, \theta)} = \frac{\beta_0 \cos\theta}{1 + \beta_0 \cos\theta} \frac{\eta_I^2 c + \alpha d}{\eta_I^2(\eta_I^2 + l^2 - m^2 - \alpha^2}, \end{aligned} \tag{45}$$

where

$$\begin{aligned}\eta_I &= 1 + \tfrac{1}{2}(a_+ + a_-),\\ l^2 &= e^2 + 2d^2,\\ \alpha &= 2cd - \tfrac{1}{2}(a_+ - a_-)\,e,\\ \beta &= -\,ce - \tfrac{1}{2}(a_+ - a_-)\,d,\\ m^2 &= \tfrac{1}{4}(a_+ - a_-)^2 + 2c^2.\end{aligned} \tag{46}$$

$a_\pm$, $c$, $d$ and $e$ have been defined earlier in (17), (19), (41) and (42). Note that the $U$ and $V$ parameters are here defined as in (5).

### 3.3. Radiative Scattering

So far we have only treated the case of true absorption. Radiative scattering has mostly been neglected when discussing the polarization in commonly used spectral lines. This neglect is made simply because the theory of scattering in a magnetic field is so complicated, but there is no physical justification for leaving scattering out. Scattering plays an important role in most absorption lines used for magnetic-field measurements. Lines formed in true absorption weaken and disappear when we pass from the centre of the disc to the limb, whereas the profile of a commonly used line such as Fe I 5250.2 Å varies only little from centre to limb.

Due to its complication, the theory of scattering has only been developed for homogeneous magnetic fields. In its general form with true absorption and coherent scattering, the transfer equation reads

$$\cos\theta \frac{d}{d\tau}\mathbf{I} = (\mathbf{1} + \boldsymbol{\eta})\,\mathbf{I} - (1 - \varepsilon)\int_{4\pi} \mathbf{S}(\gamma, \varphi; \gamma', \varphi')\,\mathbf{I}(\gamma', \varphi')\frac{d\omega'}{4\pi} - (\mathbf{1} + \varepsilon\boldsymbol{\eta})\,\mathbf{B}. \tag{47}$$

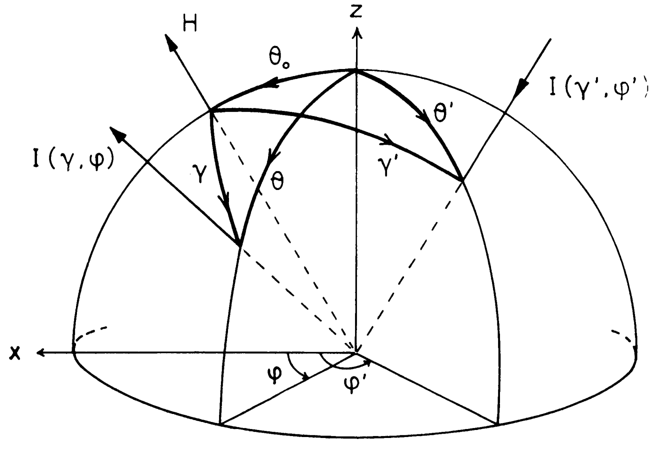


Fig. 2. Geometry for the case of radiative scattering. The $z$-axis is assumed to be normal to the stellar atmosphere. The magnetic-field vector lies in the plane made up by the $x$- and $z$-axis. $\varphi$ is the azimuth angle of the scattered ray, $\gamma$ the angle between the field and the scattered ray. $\varphi'$ and $\gamma'$ are the corresponding quantities for the incident ray.

$\mathbf{S}(\gamma, \varphi; \gamma', \varphi')$ is the scattering matrix, $\gamma'$ the angle between the incident ray and the direction of the magnetic field, $\gamma$ the angle between the scattered ray and the magnetic field, and $\varphi'$ and $\varphi$ the azimuths of the incident and scattered ray (see Figure 2). $\mathbf{I}(\gamma', \varphi')$ describes the incident radiation. It is assumed that the fraction $\varepsilon$ of the absorbed energy is transformed to thermal energy, while the rest is coherently scattered.

If the scattering is instead incoherent and we assume full redistribution of the absorbed quanta over the sublevels of the excited level, we should integrate the scattering term in (47) over all frequencies. Incoherent scattering of this kind will occur if the atom is subject to frequent collisions while it is in the excited state.

We have seen that in the case of true absorption the radiative transfer problem could be simplified considerably by diagonalizing the absorption matrix $\boldsymbol{\eta}$. When scattering is included the situation is no more that simple, because the matrices $\boldsymbol{\eta}$ and $\mathbf{S}(\gamma, \varphi; \gamma', \varphi')$ do not diagonalize simultaneously.

Stepanov (1958b, 1960a, b, c, 1962) was the first who included scattering in a theory of line formation in a magnetic field. To be able to solve the problem Stepanov made several simplifying approximations which were not physically clear. A more rigorous theory of scattering was developed by Rachkovsky (1963a, b, 1965, 1967a, b, d). Rachkovsky (1965) used the rest intensities $r_+$ and $r_-$ to compare the results from the different theories.

$$r_{\pm} = 2I_{\pm}/I_0, \tag{48}$$

where $I_{\pm}$ were defined in (32) and $I_0$ is the intensity of the continuous spectrum. The parameter $\eta_0$ was chosen independently for the different theories so that the theoretical line profile in the absence of a magnetic field at the centre of the disc should agree with the observed profile of the line Fe I 5250.2 Å. The results are shown in Figure 3 for a transversal field with $\chi = 0$ and $v_H = 1.0$. It appears that there is a quite good agreement between Rachkovsky's more rigorous and Stepanov's simplified theory, while Unno's theory gives strongly deviating results when we approach the limb. The discrepancies are as expected largest close to the line centre but become quite small far out in the wings. Hence it is necessary to use the theory of radiative scattering when calibrating solar magnetographs which use light from the centre of the line, e.g. the Locarno magnetograph.

For magnetographs working in the wings of the line it is generally not necessary to account for scattering. Unno's theory is a good approximation for $v > 1.5$ in the line wings and for the central part of the disc, i.e. for $0.7 < \cos\theta < 1$. Closer to the limb, however, it cannot be used.

In the wings for $v > 1.5$ Stepanov's theory can be used for practically the whole solar disc. For $v < 1.5$, however, the errors may be as large as 40%, and hence Rachkovsky's theory has to be used.

Rachkovsky (1963a, b, 1965) first developed the theory of scattering for atoms with a non-split upper level ($j_u = 0$), i.e. for the transition $j_l = 1$, $j_u = 0$. Obridko (1965a) found the scattering matrix for the transition $j_l = 0$, $j_u = 1$ (which we have e.g. for the line Fe I 5250.2 Å) and indicated how the scattering matrix could be found for any other transition. Rachkovsky (1967a) then developed a simple method to find the scattering matrix for arbitrary splitting of both the upper and lower levels and showed that it could be expressed as the sum of dyad products of matrices in such a way that one matrix only depends on the angle of incidence $\gamma'$ while the other only depends on $\gamma$. The equations of radiative transfer could then be integrated. It was shown (Rachkovsky, 1967d) that the problem of solving the transfer equations could be reduced to the problem of finding a solution to a system of integral equations for the generalized Ambartsumian $\varphi$ function (Ambartsumian, 1943). Obridko (1965b) on the other hand used a method by Chandrasekhar to explore his equations for the transition $j_l=0, j_u=1$.

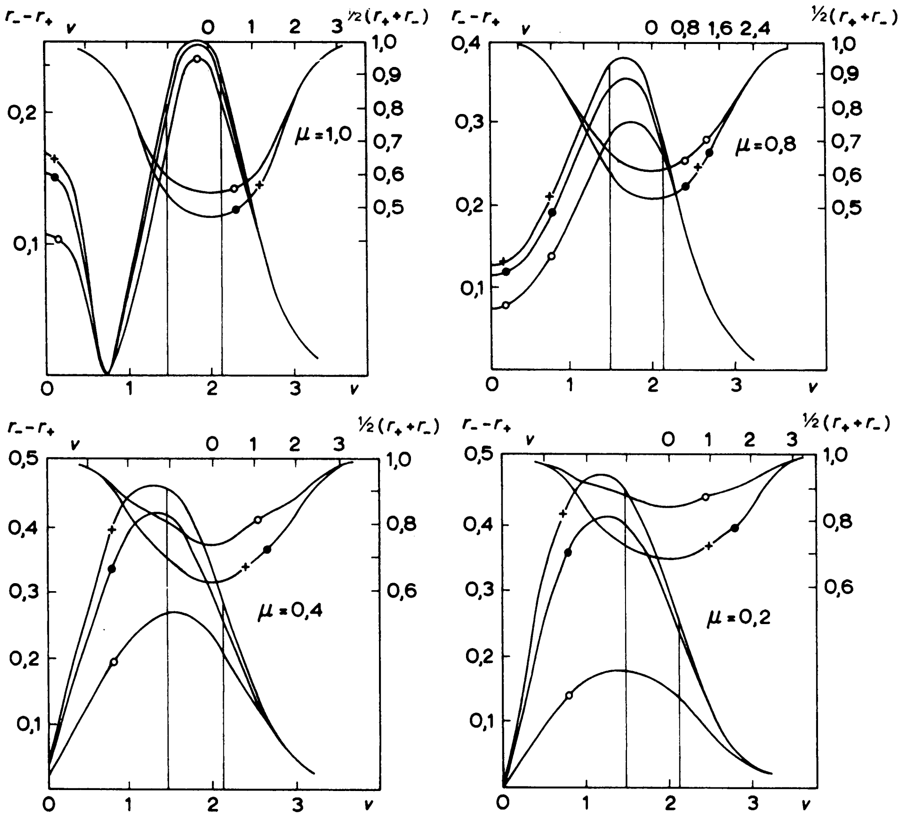


Fig. 3. Comparison according to Rachkovsky (1965) between calculations based on Rachkovsky's (filled circles) and Stepanov's (crosses) theories of scattering and Unno's (open circles) theory for true absorption. The magnetic field is assumed to be transversal with a Zeeman splitting $v_H = 1.0$. $\mu$ is the cosine of the heliocentric angle. The left and lower scales refer to $r_- - r_+$, the right and upper scales to $\frac{1}{2}(r_+ + r_-)$. The vertical lines show a typical position of an exit slit far out in the line wings. The function $r_- - r_+$ is symmetric around zero and is therefore only given for positive $v$.

Rachkovsky (1967d) also succeeded to solve the transfer equations when both anomalous dispersion and coherent scattering for arbitrary splitting were taken into account. The case of incoherent scattering was discussed in an earlier work by Rachkovsky (1963b) and has recently been treated in greater detail by Domke (1969a, b) and Rees (1969).

### 3.4. The Hanle Effect. Level-Crossing Interference

Early laboratory experiments on resonance fluorescence (Wood and Ellett, 1924; Hanle, 1924) showed how the degree of polarization and the polarization angle of the scattered light varied with the magnetic field strength and the direction and polarization of the incident radiation. The theory of these polarization phenomena, usually called the *Hanle effect*, has been developed both from the classical theory (Breit, 1925) and the quantum theory of radiation (Dirac, 1927a, b; Weisskopf, 1931; Breit, 1932, 1933).

The theory shows that when the splitting in a magnetic field is not complete so that the different sublevels overlap, they are not independent of each other but there exist phase relations between their wave functions. This interference between the sublevels is often termed *level-crossing interference.*

This level-crossing interference has simply been neglected in the theories of radiative scattering we have discussed so far. The first calculation of the scattering matrix with the interference terms included was made by Obridko (1968) for the transition $j_l=0, j_u=1$. He used the methods developed by Hamilton (1947). I have transformed Obridko's matrix to our parameter system (5). The geometry is described by Figure 2 if we put $\theta_0=0$. The scattering matrix can be conveniently written in the form

$$\mathbf{S}(\gamma, \varphi; \gamma', \varphi') = \tfrac{3}{4}[\mathbf{S}_b^{(0)} + \tfrac{1}{2}\sqrt{\eta_p}(\sqrt{\eta_r} + \sqrt{\eta_b}) \sin\gamma \sin\gamma' \mathbf{S}_i^{(1)} + \sqrt{\eta_r\eta_b}\mathbf{S}_i^{(2)} + \sqrt{\eta_p}(\sqrt{\eta_r} - \sqrt{\eta_b}) \sin\gamma \sin\gamma' \mathbf{S}_i^{(3)}], \quad (49)$$

where indices $b$ and $i$ point out that the respective matrices describe pure blending or interference effects. In earlier works only the azimuthally symmetric blending matrix $\mathbf{S}_b^{(0)}$ has been taken into account but the interference matrices $\mathbf{S}_i^{(n)}$, $n=1, 2, 3$, have been disregarded.

$$\mathbf{S}_b^{(0)} = \begin{pmatrix} 2\eta_p(1-\mu^2)(1-\mu'^2) + a_-\mu^2\mu'^2 & a_-\mu^2 & 0 & 2c'\mu^2 \\ a_-\mu'^2 & a_- & 0 & 2c' \\ 0 & 0 & 0 & 0 \\ 2c\mu'^2 & 2c & 0 & 2a_-\mu\mu' \end{pmatrix}, \quad (50)$$

where $a_-$ is obtained from (17) with $\chi=0$, i.e. $a_- = (\eta_r+\eta_b)/2$, while $c$ is given by (19). $c'$ is obtained by replacing $\gamma$ by $\gamma'$. $\mu=\cos\gamma$ and $\mu'=\cos\gamma'$.

$$\mathbf{S}_i^{(1)} = \begin{pmatrix} 4\mu\mu'\cos(\varphi'-\varphi) & 0 & 2\sqrt{2}\,\mu\sin(\varphi'-\varphi) & 0 \\ 0 & 0 & 0 & 0 \\ -2\sqrt{2}\,\mu'\sin(\varphi'-\varphi) & 0 & 2\cos(\varphi'-\varphi) & 0 \\ 0 & 0 & 0 & 2\cos(\varphi'-\varphi) \end{pmatrix}, \quad (51)$$

$$\mathbf{S}_i^{(2)} = \begin{pmatrix} \mu^2\mu'^2\cos 2(\varphi'-\varphi) & -\mu^2\cos 2(\varphi'-\varphi) & \sqrt{2}\,\mu^2\mu'\sin 2(\varphi'-\varphi) & 0 \\ -\mu'^2\cos 2(\varphi'-\varphi) & \cos 2(\varphi'-\varphi) & -\sqrt{2}\,\mu'\sin 2(\varphi'-\varphi) & 0 \\ -\sqrt{2}\,\mu\mu'^2\sin 2(\varphi'-\varphi) & \sqrt{2}\,\mu\sin 2(\varphi'-\varphi) & 2\mu\mu'\cos 2(\varphi'-\varphi) & 0 \\ 0 & 0 & 0 & 0 \end{pmatrix}, \tag{52}$$

$$\mathbf{S}_i^{(3)} = \begin{pmatrix} 0 & 0 & 0 & -\sqrt{2}\,\mu\cos(\varphi'-\varphi) \\ 0 & 0 & 0 & 0 \\ 0 & 0 & 0 & \sin(\varphi'-\varphi) \\ -\sqrt{2}\,\mu'\cos(\varphi'-\varphi) & 0 & -\sin(\varphi'-\varphi) & 0 \end{pmatrix}. \tag{53}$$

It is readily seen that

$$\mathbf{S}(\gamma,\varphi;\gamma',\varphi') = \mathbf{S}^T(\gamma',\varphi';\gamma,\varphi). \tag{54}$$

This equation expresses Helmholtz's principle of reciprocity for single scattering.

When $H \to 0$ we get $\eta_p = \eta_r = \eta_b = \eta$, $a_- = \eta$, and $c = c' = 0$. It can be directly verified that $\mathbf{S}(\gamma,\varphi;\gamma',\varphi')/\eta$ then becomes the well-known phase-matrix for Rayleigh scattering (Hamilton, 1947; Chandrasekhar, 1950).

The Doppler effect is not included in (49). Formally there is however no problem in including the Doppler effect. This is done by transforming the frequencies from a coordinate system following the atom to a system at rest and then integrate each term in (49) over the velocity distribution of the atoms. In the blending terms we obtain the well-known Voigt profiles if the velocity distribution is Maxwellian; the expressions for the interference terms will be more complicated.

If we consider a single scattering process, considerable errors may arise if the interference terms are neglected. In the transfer Equation (47), however, the light is integrated over all angles of incidence $\gamma'$ and $\varphi'$. This means that the effects of interference will be small unless the radiation field is strongly anisotropic. The latter case is present in prominences which are illuminated by light from the solar disc.

It has been shown by Rachkovsky (1964) that for the transition $j_l = 1, j_u = 0$ there will be no influence of level-crossing interference on the scattering matrix. This is the transition for the lines Fe I 6173.3 and Fe I 6302.5 Å. Spectral lines corresponding to the transition $j_l = 0, j_u = 1$ that we have discussed are the commonly used line Fe I 5250 Å, the resonance line Ca I 4227 Å, and the forbidden coronal line Fe XIII 10747 Å.

It was suggested by Hyder (1968) that the omission of the Hanle effect had caused serious errors in the interpretation of longitudinal magnetograph observations, and he calculated correction factors which should be used for the revision of the earlier measurements. These calculations were based on the assumption that the magnetic field was purely longitudinal ($\gamma = 0$). The signal from a longitudinal magnetograph is proportional to the Stokes parameter $V$. It is readily verified from (49)–(53) that the interference terms will have no contribution to the magnetograph signal. The scattered $V$ is obtained by a pure blending of the red and blue Zeeman components, as was pointed out by Stenflo (1969).

The last term in (49) describes level-crossing interference which does not occur at zero magnetic field but only at intermediate field strengths. Due to the presence of this term the statement by Lamb (1970) that the interference effects are unobservable with longitudinal magnetographs unless the incident light is at least partially circularly polarized is not entirely correct; longitudinal magnetographs may be influenced somewhat also when the incident light is linearly polarized or unpolarized.

Extensive quantum mechanical calculations of the polarization of resonance radiation in a magnetic field have been made by Lamb (1970) and House (1970a, b, 1971). Such calculations are most important not only to give a deeper understanding of the Hanle effect but also to make possible the treatment of effects which cannot be adequately handled by the classical theory, e.g. the effect of collisions.

## 4. The Zeeman Effect for Inhomogeneous Fields

It is obvious that attempts to interpret Zeeman effect measurements in terms of a homogeneous magnetic field are unrealistic. Therefore the theories discussed so far have to be generalized to treat inhomogeneous fields before they can be successfully applied to the Sun.

The importance of accounting for inhomogeneities when interpreting magnetograph observations has been pointed out by Alfvén (1952, 1967) and Alfvén and Lehnert (1956). Only recently, however, these effects have been considered in detail (Stenflo, 1966a, b, 1968a, b).

Before we start to discuss the Zeeman effect in an inhomogeneous atmosphere, we will review some general properties of solar magnetic fields.

### 4.1. Filamentary structure: general properties

A large part of the total magnetic flux on the Sun seems to emerge through small ‘flux points’ with high field strengths, while the field in between these points is quite weak. In the following we will call the regions with strong fields magnetic ‘filaments’.

Although we are presently not able to treat the filaments in a satisfactory way from the point of view of theoretical plasma physics, our knowledge about the physical conditions in solar filaments has increased significantly in recent years. Sheeley (1967) found filaments with field strengths exceeding 300 G and diameters less than one second of arc far from active regions. The location of these high field strengths coincided with strong weakenings of many spectral lines and also showed good correlation with the location of regions of $Ca^+$ $K_{232}$ emission. The intensity of the continuous spectrum was smaller and the spectral lines were generally red-shifted in the filaments. Investigating the line weakenings further, Chapman and Sheeley (1968) found that they were mainly due to more excitation and ionization in the magnetic filaments than outside them. This was explained as caused by a higher temperature in the filaments. As a consequence of the line weakenings, there is a one-to-one correspondence between the magnetic filaments and the photospheric network recorded in the same spectral line as used for the magnetic-field observations. The chromospheric network on the other hand is much coarser and shows less correlation with the photospheric magnetic field.

In a very careful study of the active region around a big unipolar sunspot, Beckers and Schröter (1968a) found more than 2000 what they called magnetic knots around the sunspot. The field strengths in the knots varied between 600 and 1400 G, and the typical diameter of a knot was 1000 km. The total magnetic flux through the magnetic knots balanced the flux through the sunspot. The knots seemed to coincide with dark intergranular regions and $Ca^+$ plages, show a generally downward flow of matter and have lifetimes exceeding 30 min. Beckers and Schröter (1968c) also found striking inhomogeneities within the umbra of the sunspot.

The weakenings of spectral lines in magnetic filaments have a serious effect on the readings of a magnetograph. The main contribution to the average line profile, which is used for calibration, comes from the interfilamentary medium. The magnetograph signal, however, is proportional to the steepness of the wings of the weakened line. Harvey and Livingston (1969) made magnetograph recordings simultaneously in different spectral lines and found large discrepancies between the results obtained. These systematic differences between the apparent field strengths obtained with the different lines could be explained entirely in terms of line weakenings of the temperature-sensitive spectral lines. Harvey and Livingston also looked for non-magnetic line weakenings in the 5250 Å line but could not find any.

If the line weakenings are caused by a temperature increase in the magnetic filaments, one would expect that the weakening depends on the field strength. Harvey and Livingston (1969) found, however, that the weakenings seemed to be independent of the recorded field strength. There seemed to be mainly two alternative interpretations of this strange result: (1) The temperature increase does not depend on magnetic-field strength if the field exceeds some small threshold value. (2) Magnetic fields outside active regions do only occur in filaments having practically one and the same field strength.

Livingston and Harvey (1969) tested the second alternative and found clear indications on what they called "quantization in photospheric magnetic flux". They determined the magnetic flux in a single filament to be $2.8 \times 10^{18}$ Mx. The diameter of a filament was not known. Assuming the cross-section to be $(1'')^2$, the field strength would be 525 G. The true cross-section might well be smaller, in which case the field strength would be correspondingly higher.

The strong temperature-sensitivity of the Fe I 5250 Å line has also been pointed out in works by Wiehr (1970) and Staude (1970b), who find that the effect is mainly caused by the low excitation potential of the lower level of the line. Wiehr (1970) suggests that the line Fe I 6302.5 Å should be suitable for magnetograph observations, since it does not change when one goes from the photosphere to the umbra of a sunspot.

Let us now consider how the line profiles are influenced by a temperature rise in the magnetic filaments. The line depth can be calculated from the equation (Gussman, 1968)

$$r_\lambda(\mu) = \int_0^\infty g(\tau, \mu)\,(1 - e^{-\tau_\lambda/\mu})\,\mathrm{d}\tau\,. \tag{55}$$

$\tau$ and $\tau + \tau_\lambda$ are the optical depths in the continuum and the line, respectively, and $\mu$ is the cosine of the heliocentric angle. The weight function is

$$g(\tau, \mu) = \frac{e^{-\tau/\mu}}{I_0(0, \mu)} \frac{\mathrm{d}B(T)}{\mathrm{d}\tau}, \tag{56}$$

where $I_0(0, \mu)$ is the intensity of the emerging radiation in the continuum, and $B(T)$ is the Planck function.

For weak lines (55) becomes

$$r_\lambda(\mu) = \frac{1}{\mu I_0(0, \mu)} \int_0^\infty e^{-\tau/\mu} \frac{\mathrm{d}B(T)}{\mathrm{d}\tau} \tau_\lambda \, \mathrm{d}\tau. \tag{57}$$

By far the most temperature-sensitive factor in the expression for $\tau_\lambda$ is the relative population number $n_{r,s}/\Sigma n_r$. This ratio between the number of atoms in excitation level $s$ and ionization stage $r$ to the total number of atoms of that element is determined by the Boltzmann and Saha equations. We can expand $\Delta n_{r,s}/\Sigma n_r$ in powers of $\Delta T/T$, but since $\Delta T/T$ is a small quantity, we need not consider higher orders than the first. If

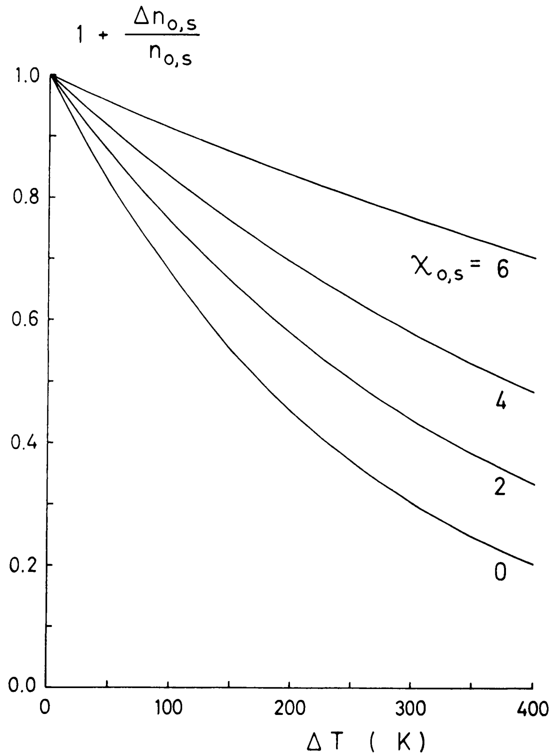


Fig. 4. The relative change in population number $n_{0,s}$ of level $s$ for neutral iron atoms as a function of the temperature increase $\Delta T$. The curves are drawn for different values of the excitation potential of level $s$ (eV).

we also assume that the change in the electron density can be neglected, we obtain for neutral metal atoms

$$1 + \frac{\Delta n_{0,s}}{n_{0,s}} \approx \exp\left[-\left(\frac{3}{2} + \frac{\chi_i - \chi_{0,s}}{kT}\right)\frac{\Delta T}{T}\right]. \tag{58}$$

In deriving (58) we have used the fact that metal atoms in the photosphere are predominantly singly ionized. $\chi_i$ and $\chi_{0,s}$ are the ionization and excitation potentials, respectively. Equation (58) is illustrated in Figure 4 for iron ($\chi_i = 7.90$ eV). If no other effect on the line profile were present, $1 + \Delta n_{0,s}/n_{0,s}$ would equal the ratio between the depths of the weakened and unweakened line, as seen from (57). The weakening is very large for low excitation potentials. The Fe I 5250 Å line has an excitation potential of only 0.12 eV, which to a large extent explains why it is so sensitive. A weakening of the same magnitude as observed by Harvey and Livingston (1969) would be obtained with $\Delta T \approx 300$ K in (58).

The proportionality between $1 + \Delta n_{0,s}/n_{0,s}$ and the line weakening is valid only in the case of weak lines. None of the lines commonly used in magnetograph observations can however be regarded as being weak, since they are not on the linear part of the curve of growth. When saturation plays a role, one has to use a larger $\Delta T$ to obtain the same weakening as for weak lines.

There is however another factor in the expression for the line depth in (55)–(57) that depends on the temperature, and that is the temperature gradient or $dB/d\tau$. If the temperature gradient is zero, the line disappears. The effect of $dT/d\tau$ depends on the level in the solar atmosphere at which the temperature rise takes place. As different lines are formed at different levels, this effect will vary from line to line.

It is possible to determine what part of the solar atmosphere that is heated by making numerical integrations of (55) for different filament models and compare the results with the observed weakenings in a great number of lines. Such a determination of the physical structure of a filament would provide an improved base for theoretical attacks on the very fundamental problem of the origin of the filaments.

### 4.2. Filamentary Structure: Interpretation of the Magnetic-Field Observations

Let us as a special case of a 'multi-stream' model of the solar atmosphere assume that we have two 'streams', one being the filaments (index $f$) and the other the interfilamentary medium (index $i$). Further we assume that the magnetograph signal is reduced in the filaments by a factor $\delta$ due to line weakening, saturation, Doppler-shift or reduced intensity. The longitudinal magnetic field in the filaments, which occupy a fraction $A_f$ of the solar surface, is $H_f$. We have corresponding notations for the interfilamentary medium. It then follows that the true average longitudinal field is

$$H = A_f H_f + A_i H_i, \tag{59}$$

while the observed average longitudinal field is

$$H_{\text{obs}} = \delta A_f H_f + A_i H_i. \tag{60}$$

If the filaments occupy only a small fraction of the solar surface, so that $A_f \ll 1$ and $A_i \approx 1$, (59) and (60) give

$$H \approx \frac{1}{\delta} H_{\text{obs}} - \frac{1-\delta}{\delta} H_i . \tag{61}$$

This is the relation between the true field and the observed field with the interfilamentary field as an unknown parameter, if we suppose that $\delta$ is known. For the mostly used line Fe I 5250.2 Å, $\delta$ has been provisionally determined by Harvey and Livingston (1969) for the central part of the solar disc, outside active regions. With the exit slits usually used in the Mt Wilson magnetograph (7–87 mÅ), $\delta$ would be 0.31, for Crimea (36–93 mÅ) $\delta \approx 0.43$.

If we use $\delta = \frac{1}{3}$, (61) becomes

$$H \approx 3H_{\text{obs}} - 2H_i . \tag{62}$$

(61) or (62) could possibly be used for the revision of all earlier magnetograph observations in the 5250 Å line. (62) is illustrated in Figure 5. One difficulty is that we

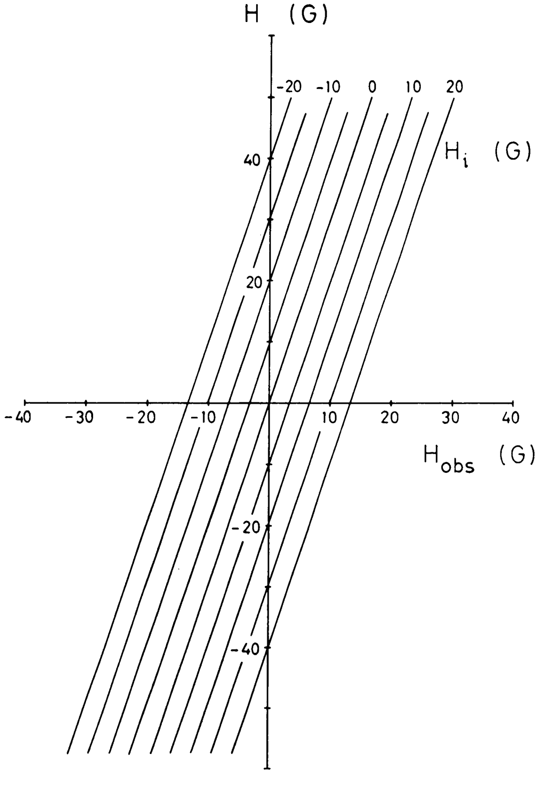


**Fig. 5.** Relation, given by (62), between the true average longitudinal field and the observed average longitudinal field (for a Babcock-type magnetograph) for a particular filamentary model with different values of the interfilamentary field strength $H_i$.

do not know $H_i$, which may have a sign opposite to the observed field. Furthermore, we do not know if $\delta$ varies across the solar disc or with the solar cycle.

Let us now turn to the case of transversal field measurements. In the observing scheme of the Crimean magnetograph, with which the pioneer work on transversal fields was done, two recordings $i_{\perp 1}$ and $i_{\perp 2}$ with different orientations of the polarization analyser are made. As was shown by Stepanov and Severny (1962), we can write

$$i_{\perp 1,2} \sim I_0 f_\perp (H) \sin^2 \gamma \begin{Bmatrix} \sin 2\chi \\ \cos 2\chi \end{Bmatrix}, \tag{63}$$

where $\chi$ is the azimuth angle of the field vector and $f_\perp (H)$ is a function that depends on the line profile and the magnetic field strength $H$. For weak fields (below a few hundred gauss), $f_\perp (H)$ is proportional to $H^2$, but it saturates and decreases again for strong fields (a few thousand gauss).

Neglecting line weakenings and fluctuations in $\gamma$ and $\chi$, the observed transversal field in the case of a multi-stream model is determined by

$$f_\perp (H_{obs}) = \sum_k A_k f_\perp (H_k). \tag{64}$$

In discussing the filamentary structure for the transversal case we will allow $A_f$ to assume any value from zero to one, but assume that the filaments carry all the flux, i.e. $H_i = 0$ and $H = A_f H_f$. We thus obtain from (64)

$$f_\perp (H_{obs}) = A_f f_\perp (H_f), \tag{65}$$

or

$$f_\perp (H/A_f) = f_\perp (H_{obs})/A_f. \tag{66}$$

For weak fields (66) reduces to

$$H = \sqrt{A_f} H_{obs}. \tag{67}$$

Hence, if the filaments occupy only a small fraction of the solar surface, the observed field strength will be much *greater* than the true field strength. If the microspots occupy 1% of the solar surface, the apparent field will be 10 times the actual field according to (67).

For larger field strengths the function $f_\perp$ saturates very quickly. Particularly this is the case for $f_\perp (H/A_f)$, when $A_f$ is small. This explains the strange behaviour of the curves in Figure 6, where we have plotted $H$ as a function of $H_{obs}$ for some different values of $A_f$. To do this the $f_\perp (H)$-curve presented by Rachkovsky (1967c) calculated according to his theory including radiative scattering has been used. All earlier transversal field measurements have been interpreted in terms of $A_f = 1$, but it is seen from Figure 6 that the interpretation is drastically changed when a filamentary structure is introduced. The observations of transversal fields exceeding 1000 G in active regions indicate however that our simplified approach is not valid there but that there must also exist, in and close to the sunspots, magnetic fields that fill up the whole space and are not merely inside narrow filaments. Nevertheless Figure 6 shows how extremely sensitive the observed transversal field is to the assumed model of the field.

https://doi.org/10.1017/S0074180900022476 Published online by Cambridge University Press

One interesting feature of Figure 6 is that it opens a new possibility to test the idea of Livingston and Harvey (1969) that the magnetic flux outside active regions is what they call 'quantized'. This case coincides with the assumptions on which Figure 6 is based. The true average field $H$ at high heliographic latitudes could be estimated from measurements of the average longitudinal field $H \cos\gamma$ assuming that the average direction of the field is along the solar radius. We assume that corrections for line weakenings are made for both the observed longitudinal and transversal fields. Close to the poles the average field will have an appreciable transversal component. Knowing

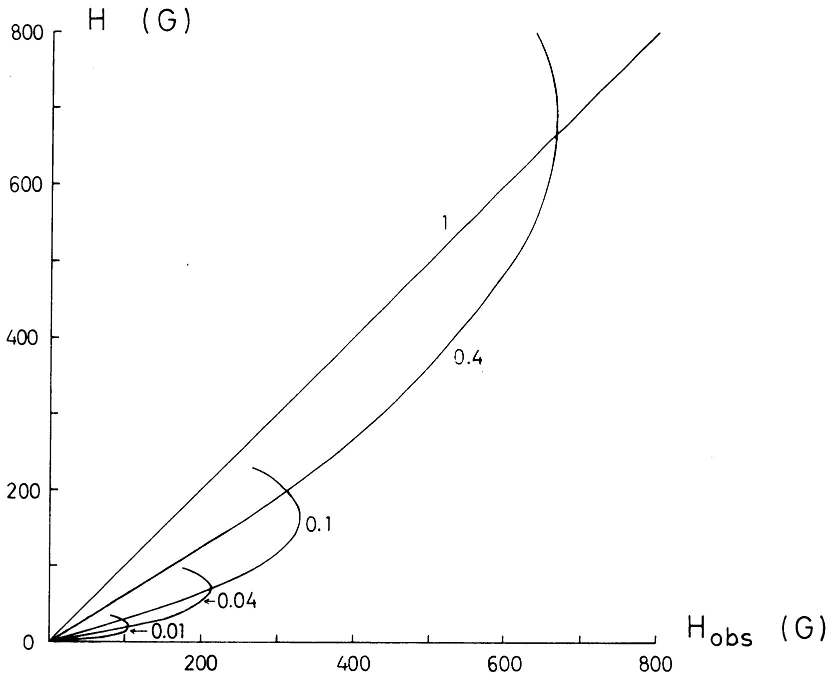


Fig. 6. Relation between the true average transversal field and the observed average field for the filamentary model described in the text. The different curves refer to the cases that 1%, 4%, 10%, 40% and 100% of the solar surface is occupied by the filaments. The last case is a homogeneous field, represented by the straight line in the figure. All earlier transversal field measurements have been interpreted with the assumption of a homogeneous field inside the scanning aperture.

$H$ the observed transversal field should be obtained from the intersection between a horizontal line in Figure 6 and the curve for the appropriate $A_f$. If $A_f = 10^{-2}$, which seems reasonable, $H = 5$ G would give $H_{obs} \approx 50$ G, and $H = 10$ G would give $H_{obs} \approx 90$ G. This is close to what should be possible to detect with transversal magnetographs by statistically reducing the noise and paying extreme attention to instrumental polarization and the position of the zero level.

### 4.3. Magnetic Microturbulence

From observations of the equivalent widths of spectral lines it can be concluded that

https://doi.org/10.1017/S0074180900022476 Published online by Cambridge University Press

there must exist a small-scale turbulence with eddies considerably smaller than 100 km having rms turbulent velocities of 1–2 km/s. As there is a coupling between the velocity field and the magnetic field in magnetohydrodynamics, one could expect that there should be fluctuations in the magnetic field on the same small scale. If there is equipartition between the magnetic and kinetic energy, the field strength should be several hundreds of gauss.

Measurements of the correlation between magnetic fields and the solar granulation have shown (Steshenko, 1960; Semel, 1962; Leighton, 1965; Livingston, 1968; Beckers and Schröter, 1968b; Howard and Bhatnagar, 1970) that if there exists any granular magnetic field at all, it cannot exceed a few tens of gauss.

The solar granulation, however, represents the long-wavelength part of the turbulence spectrum, if we at all can regard granulation as a kind of turbulence. The extremely complicated theory of hydromagnetic turbulence, which has only been developed for some idealized situations (Chandrasekhar, 1955; Kaplan, 1959; Kraichnan and Nagarajan, 1967; Nagarajan 1970, 1971), permits different solutions with different distributions of the magnetic and kinetic energies over the turbulence spectrum. Thus the magnetic energy density could be concentrated to the small eddies.

Attempts to determine the turbulent field strength of the optically thin eddies have been made (Unno, 1959; Fitremann and Frisch, 1969). The expected effects are, however, extremely small and difficult to observe, and the results that have been obtained have hardly been conclusive.

For the calculation of the polarization in spectral lines in a turbulent atmosphere we will here restrict ourselves to the special case that we only have to do with optically thin turbulent elements. In analogy with the terminology for velocity fields we will call these small-scale fluctuations in the magnetic field *magnetic microturbulence*.

An approach to a theory of magnetic microturbulence has been made by Stenflo (1968b). Staude (1970a) has also discussed the effect of microfluctuations. Ordinary microturbulence is treated by averaging the velocity-dependent terms (the absorption coefficients) in the equation of radiative transfer over a distribution of turbulent velocities. Analogously a microturbulent magnetic field may be treated by averaging the terms in the transfer equation that depend on the magnetic field over a distribution of field vectors. In the case of true absorption (14) becomes

$$\cos\theta \frac{\mathrm{d}}{\mathrm{d}t} \mathbf{I} = - \langle \kappa\varrho (\mathbf{1} + \boldsymbol{\eta}) \rangle \mathbf{I} + \langle \kappa\varrho (\mathbf{1} + \boldsymbol{\eta}) \mathbf{B} \rangle , \tag{68}$$

$t$ being the geometrical depth, $\kappa$ the coefficient of continuous absorption, and $\varrho$ the density. The averagings should be made not only over a distribution of field vectors but also over distributions of radial velocities and temperatures, as all these parameters are generally correlated in a turbulent medium. The presence of a microturbulent magnetic field may substantially change the polarization of the emerging radiation. Although it is so important, no calculations of line formation for a realistic model of a turbulent medium have yet been made.

## 5. Relations Between the Observed Magnetic Field and the Resolution of the Instrument

When the scanning aperture of a magnetograph is made smaller so that more and more of the inhomogeneities in the solar atmosphere can be resolved, one would expect that the observed average magnetic field will change. The way in which the magnetograph reading is related to the resolution is, however, far from obvious and depends strongly on the magnetograph construction and on the true structure of the magnetic field.

The first attempt to investigate the relation between the observed average field far from active regions and the slit size was made in 1965 by Stenflo (1966a, b) with the Babcock-type magnetograph of the Crimean Astrophysical Observatory. A strong increase of the observed field was found for the smallest slit size that could possibly be used then, 7 (arc s)$^2$.

The preliminary observations of the dependence on slit size were repeated one year later (Stenflo, 1968a) with the Crimean magnetograph. With a somewhat better statistical material and improvements in the magnetograph, particularly in the control of the position of the zero line, a considerably smaller increase of only about 20% for the observed average field was found for the 7 (arc s)$^2$ aperture. The systematic displacement of the zero line due to infiltration of instrumental linear polarization was found to be larger for smaller slit sizes. This could to some extent have influenced the results from 1965, when the accurate position of the zero line could not be determined (the zero line obtained with the ADP crystal switched off does not represent the true zero line for $H_{\parallel}=0$).

A theoretical investigation of the problem showed (Stenflo, 1968b) how an increase with resolution of the average field observed with a Babcock-type magnetograph is physically possible and may be caused by the better compensation of the Doppler shifts of small velocity structures. The increase with resolution will not exceed a few tens of per cent, however. It was also shown that if line weakenings occur in magnetic regions, the magnetograph will give incorrect values of the average field for any resolving power used.

The behaviour of the Evans-type magnetograph (Evans, 1964) is completely different. In contrast to the Babcock magnetograph, which has fixed exit slits and measures the intensity difference between right- and left-hand circular polarization, the Evans-type magnetograph is a servo instrument with the exit slits moving with the spectral line components, which directly determines the Zeeman splitting. If all magnetic features were resolved, the Evans-type magnetograph would give the correct field strength independently of any line weakenings that may occur.

Let us consider how the signal from an Evans-type magnetograph is influenced by the scanning aperture used in the case of a filamentary structure with the filaments evenly distributed (no clustering). We assume that the slit area is $S$, the cross-section of one filament is $S_f$, and that the filaments occupy a fraction $A_f$ of the solar surface. Further we assume that the line depth is $r(v)$ with $v=\Delta\lambda/\Delta\lambda_D$ and that the Zeeman displacement in the filaments is $v_H=\Delta\lambda_H/\Delta\lambda_D$. The spectral line is assumed to be weakened

https://doi.org/10.1017/S0074180900022476 Published online by Cambridge University Press

by a factor $\delta$ in the filaments but has the same form as the unweakened line. The magnetic field is directed along the line of sight. When *one* filament is inside the slit the magnetograph will "see" the line profile in one circular polarization $r_{\text{obs}}(v)$ determined by

$$r_{\text{obs}}(v) = \frac{S - S_f}{S}\, r(v) + \frac{S_f}{S}\, \delta r(v - v_H)\,. \tag{69}$$

The exit slits will move with this observed profile until the difference signal from the two photomultipliers is zero. The position of the exit slits then determines the observed Zeeman displacement.

The area on the sun that contains precisely one filament is $S_f/A_f$. If the slit area $S$

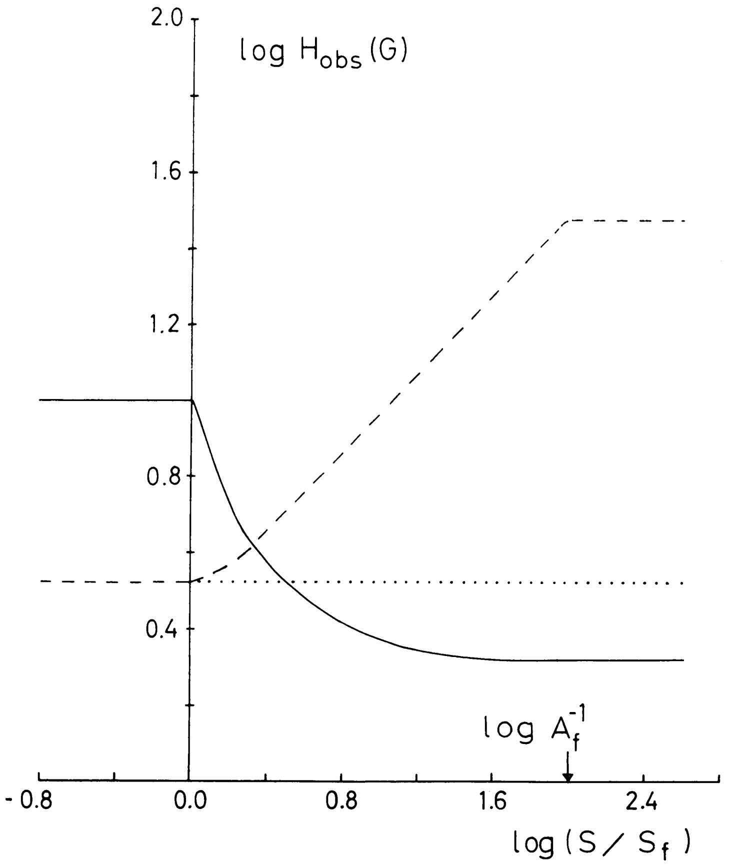


Fig. 7. Dependence of the average observed field $H_{\text{obs}}$ on the slit area $S$ for a filamentary model of the field, in which the filaments occupy a fraction $A_f = 0.01$ of the solar surface, the cross-section of a filament is $S_f$, the filamentary magnetic field is 1000 G and the interfilamentary field zero. Solid line: Evans-type magnetograph. Dotted line: Babcock-type magnetograph. Dashed line: Transversal magnetograph of the Crimean type. For the transversal field measurements it is assumed that the field in the filaments is purely transversal, for the longitudinal field measurements it is assumed that it is purely longitudinal.

is smaller than $S_f/A_f$ there will be $S_f/(SA_f)$ possible slit positions within the area $S_f/A_f$, and for all but one there is no magnetic filament within the slit. The resulting Zeeman displacement from (69) should accordingly be multiplied by $A_f S/S_f$ to give the average field strength observed with the magnetograph. The true field strength should according to this model be recorded for slits with $S \leqslant S_f$, while a considerably lower value of the field will be found for larger slits. The influence of the slit size will to some extent depend on the wavelength separation of the exit slits.

Numerical calculations of the effect have been made assuming that $r(v)$ can be described by a Gauss function and that the infinitely narrow exit slits are situated at a distance of 1.0 in the parameter $v$ from each other. Further we assume that $v_H = 1$, $A_f = 0.01$ and $\delta = \frac{1}{3}$. To give the results in G, we assume that $v_H = 1$ corresponds to a field of 1000 G in the filaments. The true average field is thus 1000 $A_f$ G = 10 G. In Figure 7 we have given $\log H_{obs}$ as a function of $\log(S/S_f)$, where $H_{obs}$ is the observed average field. The field observed with a longitudinal Babcock-type magnetograph is also illustrated (dotted line) for the same model of the field, assuming that the effects of Doppler and brightness compensations can be disregarded.

The influence of a filamentary structure on the interpretation of measurements with the transversal Crimean magnetograph was illustrated in Figure 6. The curves in this diagram have been used to calculate the dependence of the observed transversal magnetic field on the slit area $S$ in our filamentary model. The result is presented in Figure 7.

It appears from Figure 7 that the observed average field shows an entirely different dependence on the slit area in the three cases. If such relations between $H_{obs}$ and $S$ could be determined empirically, it would be possible not only to test the assumption of a filamentary structure but also to obtain information on the important parameters $S_f$, $A_f$ and $H_f$.

## 6. Conclusive Remarks. Suggestions for the Future

Obviously there is still much to be done before we can correctly interpret what is measured with a magnetograph. But our insight in the problems has increased significantly during the last years, and we are beginning to reveal the nature of the filamentary structure of the solar atmosphere.

As a kind of summary some recommendations and suggestions for future work in this field will be listed.

(1) The line Fe I 5250.2 Å should not be used further in magnetograph observations because it is so temperature-sensitive. The suitability of other lines should be thoroughly investigated.

(2) All earlier observations in the line Fe I 5250.2 Å should be revised. To do this we need to know the relation between the filamentary and interfilamentary fields. The variation of the line weakenings over the solar disc and with the solar cycle should also be determined.

(3) The filamentary nature of the field could be tested and studied by making recordings with different slit sizes with a Babcock-type, Evans-type and a transversal

https://doi.org/10.1017/S0074180900022476 Published online by Cambridge University Press

magnetograph. This could give information on the size and distribution of the filaments.

(4) A physical model (mainly temperature stratification) of a filament could be established by recording the magnetic field in a great number of spectral lines, which are weakened differently in the filaments.

(5) Earlier interpretations of transversal field measurements should be reexamined by making recordings of the transversal field in *active regions* with different slit sizes.

(6) The theory of line formation in a magneto-turbulent medium should be further developed. The polarization in the lines should be calculated for a realistic turbulent model in which the different physical parameters are coupled to each other.

(7) Numerical calculations of the effect of level-crossing interference on measurements of prominence magnetic fields should be made.

Of course this list of suggestions is very incomplete, but nevertheless it illustrates how much there is to be done. All our knowledge of solar magnetic fields is based on the theory we use to interpret the observations, and it is no wonder that this theory has received so much attention during the last years.

## References


Alfvén, H.: 1952, *Arkiv Fysik* **4**, 407.

Alfvén, H.: 1967, in *Magnetism and the Cosmos* (ed. by Hindmarsh, Lowes, Roberts, and Runcorn), Oliver & Boyd, Edinburgh/London, p. 246.

Alfvén, H. and Lehnert, B.: 1956, *Nature* **178**, 1339.

Ambartsumian, V. A.: 1943, *Dokl. Akad. Nauk S.S.S.R.* **38**, No. 8.

Beckers, J. M.: 1969a, *Solar Phys.* **9**, 372.

Beckers, J. M.: 1969b, *Solar Phys.* **10**, 262.

Beckers, J. M. and Schröter, E. H.: 1968a, *Solar Phys.* **4**, 142.

Beckers, J. M. and Schröter, E. H.: 1968b, *Solar Phys.* **4**, 165.

Beckers, J. M. and Schröter, E. H.: 1968c, *Solar Phys.* **4**, 303.

Born, M.: 1965, *Optik*, 2nd ed., Springer-Verlag, New York.

Breit, G.: 1925, *J. Opt. Soc. Am.* **10**, 439.

Breit, G.: 1932, *Rev. Mod. Phys.* **4**, 504.

Breit, G.: 1933, *Rev. Mod. Phys.* **5**, 91.

Chandrasekhar, S.: 1950, *Radiative Transfer*, Clarendon Press, Oxford.

Chandrasekhar, S.: 1955, *Proc. Roy. Soc. London* **233**, 322 and 390.

Chapman, G. A. and Sheeley, Jr., N. R.: 1968, *Solar Phys.* **5**, 442.

Dirac, P. A. M.: 1927a, *Proc. Roy. Soc. London* **114**, 710.

Dirac, P. A. M.: 1927b, *Proc. Roy. Soc. London* **114**, 243.

Domke, H.: 1969a, *Astrofiz.* **5**, 525.

Domke, H.: 1969b, *Monatsber. Deut. Akad. Wiss. Berlin* **11**, 269.

Evans, J. C.: 1968, Report at the MASUA Theoretical Physics Conference, University of Nebraska, Nov. 2–3, 1968.

Evans, J. C.: 1969a, Report at the Special Meeting on Solar Astronomy of the AAS, Pasadena, Febr. 18–21, 1969.

Evans, J. C.: 1969b, Report at the IAU Symposium on Laboratory Astrophysics, York University, Toronto, Ontario, Canada, Nov. 7–8, 1969.

Evans, J. C. and Dreiling, L. A.: 1969, Report at the 130th Meeting of the AAS, State University of New York, Albany, New York, Aug. 11–14, 1969.

Evans, J. W.: 1964, in *Atti del Convegno sui Campi Magnetici Solari* (ed. by G. Barbèra), Firenze.

Fitremann, M. and Frisch, U.: 1969, *Compt. Rend. Acad. Sci. Paris* **268**, 705.

Gussman, E. A.: 1967, *Z. Astrophys.* **65**, 456.

Hamilton, D. R.: 1947, *Astrophys. J.* **106**, 457.
Hanle, W.: 1924, *Z. Phys.* **30**, 93.
Harvey, J. and Livingston, W.: 1969, *Solar Phys.* **10**, 283.
House, L. L.: 1970a, *J. Quant. Spectr. Radiative Transfer* **10**, 909.
House, L. L.: 1970b, *J. Quant. Spectr. Radiative Transfer* **10**, 1171.
House, L. L.: 1971, *J. Quant. Spectr. Radiative Transfer* **11**, 367.
Howard, R. and Bhatnagar, A.: 1969, *Solar Phys.* **10**, 245.
Hyder, C. L.: 1968, *Solar Phys.* **5**, 29.
Kai, K.: 1968, *Publ. Astron. Soc. Japan* **20**, 154.
Kaplan, S. A.: 1958, in *Electromagnetic Phenomena in Cosmical Physics* (ed. by B. Lehnert), Cambridge University Press, p. 504.
Kraichnan, R. H. and Nagarajan, S.: 1967, *Phys. Fluids* **10**, 859.
Lamb, F. K.: 1970, *Solar Phys.* **12**, 186.
Leighton, R. B.: 1965, in R. Lüst (ed.), 'Stellar and Solar Magnetic Fields', *IAU Symp.* **22**, 158.
Livingston, W.: 1968, *Astrophys. J.* **153**, 929.
Livingston, W. and Harvey, J.: 1969, *Solar Phys.* **10**, 294.
Mattig, W.: 1966, in *Atti del Convegno sulle Macchie Solari* (ed. by G. Barbèra), Firenze.
Moe, O. K.: 1968, *Solar Phys.* **4**, 267.
Moe, O. K. and Maltby, P.: 1968, *Astrophys. Letters* **1**, 189.
Nagarajan, S.: 1970, *Phys. Fluids*, in press.
Nagarajan, S.: 1971, this volume, p. 487.
Obridko, V. N.: 1965a, *Astron. Zh.* **42**, 102.
Obridko, V. N.: 1965b, *Astron. Zh.* **42**, 502.
Obridko, V. N.: 1968, *Soln. Aktivnostj* No. 3, 64.
Rachkovsky, D. N.: 1961a, *Izv. Krymsk. Astrofiz. Obs.* **25**, 277.
Rachkovsky, D. N.: 1961b, *Izv. Krymsk. Astrofiz. Obs.* **26**, 63.
Rachkovsky, D. N.: 1962a, *Izv. Krymsk. Astrofiz. Obs.* **27**, 148.
Rachkovsky, D. N.: 1962b, *Izv. Krymsk. Astrofiz. Obs.* **28**, 259.
Rachkovsky, D. N.: 1963a, *Izv. Krymsk. Astrofiz. Obs.* **29**, 97.
Rachkovsky, D. N.: 1963b, *Izv. Krymsk. Astrofiz. Obs.* **30**, 267.
Rachkovsky, D. N.: 1965, *Izv. Krymsk. Astrofiz. Obs.* **33**, 111.
Rachkovsky, D. N.: 1967a, *Izv. Krymsk. Astrofiz. Obs.* **36**, 3.
Rachkovsky, D. N.: 1967b, *Izv. Krymsk. Astrofiz. Obs.* **36**, 9.
Rachkovsky, D. N.: 1967c, *Izv. Krymsk. Astrofiz. Obs.* **36**, 51.
Rachkovsky, D. N.: 1967d, *Izv. Krymsk. Astrofiz. Obs.* **37**, 56.
Rees, D. E.: 1969, *Solar Phys.* **10**, 268.
Semel, M.: 1962, *Compt. Rend. Acad. Sci. Paris.* **254**, 3978.
Severny, A. B.: 1964, *Izv. Krymsk. Astrofiz. Obs.* **31**, 126.
Severny, A. B.: 1965, *Izv. Krymsk. Astrofiz. Obs.* **33**, 3.
Sheeley, Jr., N. R.: 1967, *Solar Phys.* **1**, 171.
Staude, J.: 1970a, *Solar Phys.* **12**, 84.
Staude, J.: 1970b, *Solar Phys.* **15**, 102.
Stenflo, J. O.: 1966a, *Observatory* **86**, 73.
Stenflo, J. O.: 1966b, *Arkiv. Astron.* **4**, 173.
Stenflo, J. O.: 1968a, *Acta Univ. Lund.* II No. 1 (= *Medd. Lunds Astron. Obs.* Ser. II Nr: 152).
Stenflo, J. O.: 1968b, *Acta Univ. Lund.* II No. 2 (= *Medd. Lunds Astron. Obs.* Ser. II Nr: 153).
Stenflo, J. O.: 1969, *Solar Phys.* **8**, 260.
Stepanov, V. E.: 1958a, *Izv. Krymsk. Astrofiz. Obs.* **18**, 136.
Stepanov, V. E.: 1958b, *Izv. Krymsk. Astrofiz. Obs.* **19**, 20.
Stepanov, V. E.: 1960a, *Izv. Krymsk. Astrofiz. Obs.* **23**, 291.
Stepanov, V. E.: 1960b, *Izv. Krymsk. Astrofiz. Obs.* **24**, 293.
Stepanov, V. E.: 1960c, *Astron. Zh.* **37**, 631.
Stepanov, V. E.: 1962, *Izv. Krymsk. Astrofiz. Obs.* **27**, 140.
Stepanov, V. E. and Severny, A. B.: 1962, *Izv. Krymsk. Astrofiz. Obs.* **28**, 166.
Steshenko, N. V.: 1960, *Izv. Krymsk. Astrofiz. Obs.* **22**, 49.
Unno, W.: 1956, *Publ. Astron. Soc. Japan* **8**, 108.

Unno, W.: 1959, *Astrophys. J.* **129**, 375.
Weisskopf, V.: 1931, *Ann. Phys.* **9**, 23.
Wiehr, E.: 1970, *Solar Phys.* **11**, 399.
Wood, R. W. and Ellett, A.: 1924, *Phys. Rev.* **24**, 243.

## Discussion

*Pecker:* (1) For *numerical* purposes, in small magnetic fields the Stokes parameters $I$ and $Q$ are more useful than the $I_1$ and $I_2$, which are convenient in the algebraic treatment. One actually needs to know accurately $Q$, not $I$ (this being a comment valid for weak fields, of course!).

(2) It is clear that in *weak* fields, the coupling of magnetic effects and source function is essential; one cannot use a source function of 'fine scattering' when depolarizing collisions are quite essential!

(3) Would the *ionized iron* lines be a better choice than the neutral iron lines often in use, as they are less temperature dependant?

*Stenflo:* The main reason why the line Fe I 5250 Å is so temperature sensitive is the low excitation potential of the lower level, 0.12 eV. A small temperature change will cause a large change in the population number of that level. Ionized lines may be better, but are also affected by temperature changes. One should carefully investigate the behavior of different lines to find the most suitable one for magnetograph observations.

*Athay:* If I understand correctly, the scattering is treated coherently. This is incorrect, of course, since the scattering is actually incoherent. Could you comment on the effect of the incoherence. Secondly, the presence of velocity fields in the Sun generally makes the lines asymmetric. Could you comment on this effect.

*Stenflo:* The case of incoherent scattering has been treated by Rachkovsky and Domke, but as far as I know, nobody has made quantitative estimates of how much the results will differ from the case of coherent scattering. The effect of asymmetry of the line profile on the magnetograph recordings is always present but is very small compared with the other effects I have discussed.

*Schatten:* Observations of the interplanetary magnetic field have been compared with the photospheric magnetic field as measured by magnetographs by Wilcox and Ness, Schatten *et al.*, and Severny *et al.* They have shown that the 'mean' photospheric field agrees with the observed interplanetary field both in polarity and in *magnitude*. The agreement is probably accurate to about 80%. Thus it is difficult to reconcile the factor of 3 weakening in field strength in the magnetograph observations as you suggest. I would like to know your comments on this problem.

*Stenflo:* As I see it the really significant results you mentioned is the excellent correlation between the *polarities* of the solar and interplanetary magnetic fields. The polarity pattern on the Sun will probably not be changed when taking into account the line weakenings in the magnetic filaments. The establishment of the relation between the *magnitudes* of the solar and interplanetary magnetic fields is not so certain, and I think one has to reexamine this problem again.

*Michard:* I suggest that tests of the influence of an unresolved fine structure of magnetic fields on measured averages, can best be made by the simultaneous study of lines with different Zeeman patterns: these will be differently influenced by the fine structures.

*Stenflo:* There are many ways in which the influence of the fine structure may be studied. In addition to the suggestion by Dr Michard, one of the best methods would be to make magnetograph recordings in a great number of lines of different temperature-sensitivity to determine what layers of the solar atmosphere are heated.

*Wiehr:* Fe $\lambda$ 5250 can *not* be replaced by an Fe+ line since the latter one shows the opposite behavior to Fe $\lambda$ 5250. This was shown by Harvey and Livingston for the filamentary structures and by myself for sunspots. One should use a 3.5 eV line like Fe $\lambda$ 6303.

*Stenflo:* Even the Fe $\lambda$ 6303 Å line seems to be affected by the temperature increase in the filaments.

*Lamb:* I would like to make a brief comment concerning the effects of collisional depolarization. Although collisional depolarization is expected to be quite important in the lower regions of the solar atmosphere, there are strong theoretical reasons for expecting that the rate of collisional depolarization will not depend on magnetic field strength for fields of less than $5 \times 10^3$ G.

*Deubner:* Can you give theoretical arguments why the filamentary structure should be so pronounced as you mentioned, using values down to 1% of the total area being occupied by magnetic field strands in order to estimate the ratio of $H_{\rm obs}$ to the true field strength $H$? E.g. yesterday we learned from Livingston's high resolution magnetograms that there are magnetic fields evenly distributed all over the solar surface.

*Stenflo:* Unfortunately there is no theory that can satisfactorily explain why the filamentary structure is so pronounced. The observations by Livingston and Harvey indicate that most of the total magnetic flux is 'channelled' through these narrow filaments. At the same time they observe weak fields of more or less random distribution in between the filaments. The theoretical relation between the filamentary and interfilamentary magnetic fields is not clear, and we do not know how large a part of the total flux is in the interfilamentary medium.

*Dunn:* Let us not encourage people to duplicate the Evans type of magnetograph. You see it follows the center of gravity of one of the components and the $\pi$ component. Thus in the presence of a $\pi$ component it becomes a longitudinal type magnetograph. With no $\pi$ component it measures total field. So in a weak sunspot it measures longitudinal field. As the spot strengthens the slits may jump between the $\pi$ component and $\sigma$ component. Years ago I tried to solve this problem by chopping between the continuum and the edge of the line. The noise went up but it was a successful solution, however it did not really appear practical for daily mapping. I think an equally good but simpler solution is a two channel Babcock magnetograph operating on a weakly and strongly split line, or perhaps one of the magnetographs described here that measure the Stokes' parameters, or one that records the entire line profile.

*Stenflo:* I think all types of magnetographs are most valuable, because from their different behavior in the presence of a filamentary structure, we can learn about the unresolved fine structure of the magnetic field.

*Severny:* We have not been able to find out outside of active regions such a drastic change in the line profile $\lambda$ 5250 as was found at Kitt Peak. Perhaps the resolution in our observations ($2'' \times 4''$) was not as good as at Kitt Peak, but it is still quite adequate for such a search of fine structure. Especially for polar regions we were not able to find results like that found at Kitt Peak regarding the line profile of $\lambda$ 5250. I have no doubt that inside active regions we have such an effect of decrease of the steepness of $\lambda$ 5250, but I am not sure that this takes place also for the regions of general field outside active regions. So that I think we should consider the statement that we should change all our measurements on $\lambda$ 5250 by a factor of 3 with some reserve.